

RAINFALL SPATIAL VARIABILITY OBSERVED BY X-BAND WEATHER RADAR AND ITS IMPLICATION FOR THE ACCURACY OF RAINFALL ESTIMATES

Emmanuel Moreau^{1*}, Jacques Testud² and Erwan Le Bouar¹,
¹ NOVIMET, Vélizy, France
² LATMOS/CNRS, velizy, France

1. INTRODUCTION

The main objective of this paper is to estimate the error in the rainfall derived from a polarimetric X-band radar, by comparison with the corresponding estimate of a rain gauge network. However the present analysis also considers the errors inherent to raingauge, in particular instrumental and representativeness errors. A special emphasis is addressed to the spatial variability of the rainfall in order to appreciate the representativeness error of the rain gauge with respect to the 1km square average, typical of the radar derived estimate. For this purpose the spatial correlation function of the rainfall is analyzed.

The data set consists of one-year radar data collected by the X-band polarimetric radar HYDRIX®, located in Beauce region (80km south of Paris). All data were processed in real time using the ZPHI® algorithm. A dense rain gauge network provided ground comparison data. The various sources of uncertainties (instrumental and representativeness) are then analyzed and quantified for each sensor.

2. EXPERIMENTAL SETUP

The radar data used in this study comes from an X band dual polarization radar (named HYDRIX). This "compact" radar (antenna diameter is 1.2 m) uses the hybrid technology (i.e. simultaneous transmission of H&V polarizations).

The HYDRIX radar was deployed on October 2004, on the roof of a building of the Arvalis-Institut-du-Végétal, an agricultural institute located 70 km south of Paris, France. To validate the measurements of the HYDRIX radar, a network of 24 rain gauges was specially deployed in the azimuth sector covered by the radar, within 25 km range. The radar scanning zone is a single elevation azimuth sector spanning from 200° to 275°, with a maximum range of 60 km. The 3 deg/s antenna speed ensures a revisit time less than 30 s long in average. During the reference period October 2004 to October 2005, the radar produced 14745 estimates of the six-minute rainfall over the 24 rain gauges of the network, representing a total rainfall of 307 mm (average at each rain gauge site).

The HYDRIX radar data was processed in real time with the ZPHI® algorithm (Testud et al., 2000) to retrieve the rain rate and the parameter N_0^* of the

drop size distribution (Testud et al., 1999). The latter helps to adjust the reflectivity (Z) – rainfall rate (R) relationship to the meteorological situations. The radar rain rates were then interpolated in a 1 km² resolution geographic grid, using Cressman filtering. They were also time integrated primarily over 6 mn to fit the rain gauge time sampling.

Two other algorithms are used for comparison purpose, a classical Z-R relationship with and without attenuation correction from ZPHI®. In both cases the N_0^* is set to a constant value optimized for the region ($\sim 10^{6.4} \text{ m}^{-4}$).

3. RADAR ALGORITHM COMPARISON

Table 1 summarizes the statistics of the point-by-point comparison of the hourly rainfall measured by the rain gauges and by the radar during the reference period. Statistics are computed in terms of Pearson correlation coefficient, Nash criterion and slope of the orthogonal regression function.

Compared to rain gages, the classical Z-R estimator is negatively biased, especially for higher rainfall, due to attenuation. The Pearson correlation coefficient and the Nash criterion are substantially improved not only with respect to the "classical Z-R", but also with respect to the "attenuation corrected Z_c -R". The performance of ZPHI® is due to two factors: first, the relationship between specific attenuation and rain rate is naturally less scattered than the Z-R relationship, and second, the ray-by-ray adjustment of N_0^* allows the effect of the natural variability of the DSD to be considerably reduced.

Algo	Slope	Pearson	Nash
ZPHI®	0.88	0.92	0.84
R(Z_{corr})	1.09	0.85	0.66
R(Z_{att})	0.68	0.80	0.62

Table 1. Statistics of the comparison between radar and gauges, 3652 points, 1hour integration.

4. RAIN VARIABILITY OBSERVED BY RADAR AND GAUGES

A spatial correlation analysis has been carried out to characterize the rain variability based on the procedure described by Gebremichael and Krajewski (2004) (GK2004 hereafter).

First the spatial correlation of gauge and

* Corresponding author address: Emmanuel Moreau
 Novimet, 10-12 av. de l'europe 78140 Vélizy,
 France ; email : emmanuel.moreau@novimet.com

collocated radar data are computed, for 6min rain accumulation, assuming a lognormal distribution.

Then, the gauge spatial correlation is fitted by the exponential point-correlation function:

$$\rho(h) = \rho_0 \exp\left(-\left(h/R_0\right)^F\right) \quad (1)$$

where h is the separation distance, F is the shape parameter, R_0 is the correlation radius (km), and ρ_0 defines the nugget parameter. The nugget parameter is the local decorrelation that can be caused by microscale variability or by random instrumental errors. A standard least square fit routine is used to adjust the shape parameter F and the correlation radius R_0 for determining the best fit to the experimental points. The minimum distance between the gauges in the network was not small enough ($>1.2\text{km}$) to accurately determine the nugget parameter. The nugget parameter is fixed to 0.97 by default for all cases.

Finally, the radar spatial correlation is fitted by the area-correlation function ρ_A using a Gradient-expansion nonlinear least square algorithm:

$$\rho_A(h) = \text{cov}_A[h] / \text{var}[R_A(x, y)] \quad (2)$$

where the variance and covariance of the area average rain field $R_A(x, y)$ is a function of the three-parameter exponential point correlation $\rho(h)$

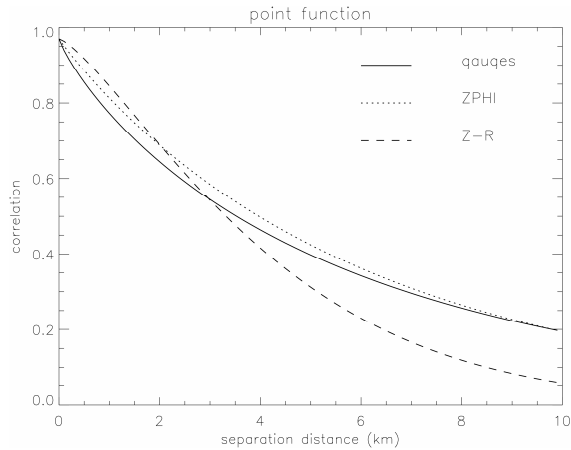


Fig. 1: The "point" correlation functions derived from the three data sources: the 24-rain gauge network, the ZPHI® radar and the classical Z-R radar estimate.

GK2004 observed that the correlation function determined from the radar dropped faster (meaning a shorter correlation radius) than the one determined from the rain gauge network. A similar observation can be made when comparing the "classical Z-R" correlation function with the rain gauge one (Fig 1). However, the correlation function for ZPHI® rainfall estimate turns out to be very close to the one for the rain gauge network (Fig 1). Such a result constitutes an independent way to validate the ZPHI® product in comparison with the rain gauge network.

From the radar alone, thanks to the large number of available samples, an accurate correlation function may be derived from one month of hourly rainfall data

(Figure 2). We notice the almost perfect fit of the area correlation function ρ_A over the radar data. From the spatial area correlation $\rho_A(h)$ (eq. 2), one can deduce the spatial point correlation function $\rho(h)$ (i.e. the one that would be obtained from rain gauge measurements). The latter, also plotted in Figures 2 exhibits lower correlations up to 8km separation distance. The large reduction is observed at short distances and for the more convective events. The correlation radius decreases rapidly when considering only higher rainfall rates, R_0 drops from 31km to 6.5km when selecting rain rates higher than 3mm/h.

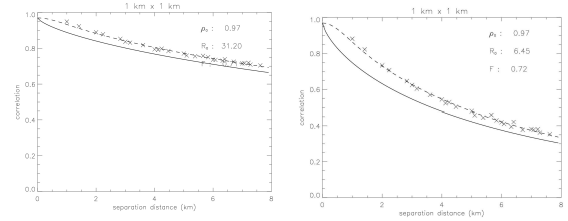


Fig. 2: spatial correlation derived from one month (October 2004) of 1hr rain retrieved from radar measurements by ZPHI®. The fitted function $\rho_A(h)$ and $\rho(h)$ are represented by the dash and the solid line respectively. All rainfall rates (on the left). Rainfall rates higher than 3 mm/h (on the right).

5. INSTRUMENTAL AND REPRESENTATIVENESS ERRORS

As mentioned before, direct comparisons of gauge and radar estimates are problematic because of the large differences in their sampling volumes. The gauge represents only a small fraction of the sampling volume of the radar; $\sim 0.1 \text{ m}^2$ versus 1 km^2 for the HYDRIX data.

We define the instrumental error A_{rad} attached to the radar, by:

$$R_{rad} = A_{rad} R \quad (3a)$$

and for the gauge error B_g related to bucket sampling, by:

$$R_g = r + B_g \quad (3b)$$

where R_{rad} denotes the radar-rainfall estimates over the area A (1 km^2) and R_g the gauge rainfall at a certain point within the area, r stands for the true point rainfall, R the true area-averaged rainfall defined by:

$$R = \int_A r dx$$

The error A_{rad} is assumed multiplicative, independent of the rainfall intensity, lognormally distributed. The hypothesis that A_{rad} is in addition independent of R means that the relative error is constant (hence the absolute error grows proportionally to R). We are conscious that this hypothesis of independence is imperfect and mainly dictated by convenience to perform the calculation. But it is probably the best we can do with our present knowledge. Similarly, it is assumed that the error B_g ,

additive and normally distributed, is independent of the rainfall intensity. B_g is an absolute error representing the resolution of the tipping bucket (0.2mm). All previously defined errors are assumed not biased. More details on the instrumental errors can be found in Moreau et al. (2009).

The standard error for is defined as follows:

$$\varepsilon_{rad-inst} = \sqrt{\text{var}(A_{rad})} \quad (4)$$

As the error in the rain gauge estimate is absolute, in order to be able to compare it with the radar estimate, a normalization is practiced as:

$$\varepsilon_{g-inst} = \sqrt{\frac{\text{var}(B_g)}{E(r^2)}} \quad (5)$$

with $\text{var}(B_g) = (0.2 \text{ mm/h})^2$

ε_{g-inst} is referred to in the following as the "relative error" in the raingauge estimate.

Similarly, the normalized representativeness error is defined by:

$$\varepsilon_{rep} = \sqrt{\frac{\text{var}(r - R)}{E(R^2)}} \quad (6)$$

where $E(\cdot)$ and $\text{var}(\cdot)$ are the expectation and variance operators, respectively.

The point-area difference variance divided by the point variance can be expressed, as in Ciach and Krajewski (2002), by:

$$\frac{\text{var}(r - R)}{\text{var}(r)} = 1 - \frac{2}{A} \rho_0 \int_A \tilde{\rho}(x, x_g) dx^2 \quad (7a)$$

$$+ \frac{1}{A^2} \rho_0 \iint_A \tilde{\rho}(x, y) dx^2 dy^2 = 1 - 2f_3 + f_1$$

and

$$\text{var}(R) = \text{var}(r) f_1 \quad (7b)$$

$$\text{cov}(r, R) = \text{var}(r) f_3$$

where x_g denotes the location of the gauge within the area and $\text{cov}(\cdot)$ is the covariance operator. The point correlation function $\tilde{\rho} = \rho / \rho_0$ denotes the spatial correlation assuming no local decorrelation. The nugget parameter reflects the microscale variability in the rain fields and the random measurement errors of the rain gauges. As mentioned before, the rain gauge network used in this study is not dense enough to accurately estimate this parameter from the spatial correlation. Therefore, the nugget parameter is left as a free parameter that would be estimated.

The variance of the difference between the rain-radar and the rain-gauge can be expressed as:

$$\text{var}(R_g - R_{rad}) = \text{var}(R_g) + \text{var}(R_{rad}) - 2\text{cov}(R_g, R_{rad}) \quad (8)$$

The last term in eqn (8), the covariance between the rain-radar and the rain-gauge, can be written as:

$$\text{cov}(R_g, R_{rad}) = E(R_g \cdot R_{rad}) - E(R_g)E(R_{rad}) \quad (9)$$

Substituting R_g and R_{rad} by eqn (3a) and (3b) and considering that errors are not biased and independent of the rainfall, leads to:

$$\text{cov}(R_g, R_{rad}) = E(rR) - E(r)E(R) = \text{cov}(r, R) \quad (10)$$

The covariance between the point and the area-average rainfall can be estimated by substituting eqn (8) into (10).

Using eqns (7a) and (7b), the variance of the area-average rainfall can be written as:

$$\begin{aligned} \text{var}(R) &= \text{cov}(r, R) \frac{f_1}{f_3} \\ &= \text{cov}(r, R) \frac{\frac{1}{A^2} \iint_A \tilde{\rho}(x, y) dx^2 dy^2}{\frac{1}{A} \int_A \tilde{\rho}(x, x_g) dx^2} \end{aligned} \quad (11)$$

It has to be noticed that eqn (11) is totally independent of the nugget parameter. The variance of the point rainfall is deduced, by expressing the variance of eqn (3b), as:

$$\text{var}(r) = \text{var}(R_g) - \text{var}(B_g) \quad (12)$$

Finally, the nugget parameter can be derived by substituting eqns (13) and (14) into eqn (7b) :

$$\rho_0 = \frac{\text{var}(r)}{\text{var}(R)} = \frac{\text{var}(r)}{A^2 \iint_A \tilde{\rho}(x, y) dx^2 dy^2} \quad (13)$$

The normalized representativeness ε_{rep} error can be estimated substituting eqns (12) and (13) into eqn (6). The normalized instrumental radar error $\varepsilon_{rad-inst}$ can be derived, by expressing the variance of eqn (3a):

$$\varepsilon_{rad-inst}^2 = \text{var}(A_{rad}) = \frac{\text{var}(R_{rad}) - \text{var}(R)}{E(R^2)} \quad (14)$$

The inputs to this approach are the variances of the observed radar rain estimate and gauge rain estimate, as well as the variance of their difference, and finally the point correlation function. The point correlation function $\tilde{\rho}$ (assuming no instant decorrelation) is derived from the 1-hr rain radar data (Figure 2) when a rain threshold of 1mm/h (or 2 mm/h) is applied, the nugget parameter ρ_0 being estimated through eqn (13).

As mentioned before all rain measurements are assumed unbiased. The bias is estimated from the data set, from the slope of the orthogonal regression and removed from the radar rain measurements. The rain gauge data are assumed not biased.

The error analysis is applied to the one year data set for 1 hour integration time. On figure 3 are displayed: the sample number (a), the Pearson correlation of radar versus gauge rain (b), the bias (c), the instrumental and representativeness gauge errors (d), the radar error (e).and the nugget parameter (f).

The robustness of the error analysis to the hypothesis of independent errors is tested by applying different rain thresholds (from 0 mm/h to 2.0 mm/h) to the dataset. Larger rain thresholds reduce considerably the sample number leading to an unstable analysis.

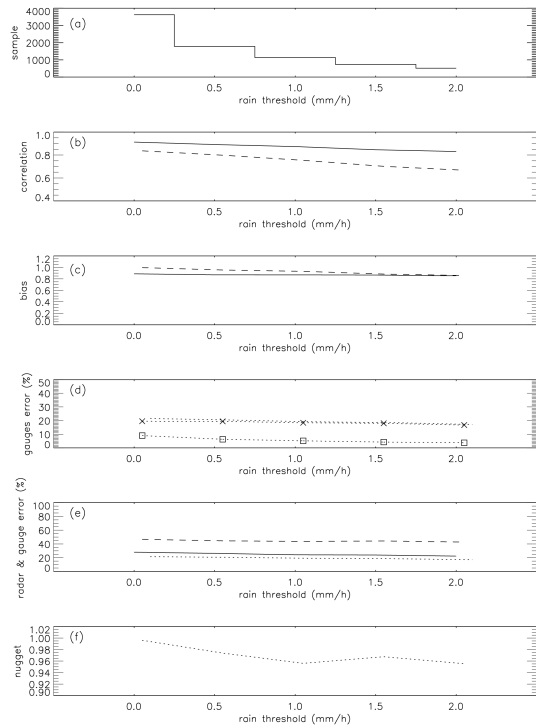


Fig 3: error analysis of the one year rain data set. In all the panels, the statistics associated to ZPHI® are in solid line (---), to the attenuation corrected “Z_c-R” algorithm in dashed line (---) and to the gauges in dot line (...). From the top to the bottom; (a) the sample number used to derive the statistics; (b) the Pearson correlation coefficient; (c) the bias; (d) the instrumental (ϵ_{g-inst}) and representativeness (ϵ_{rep}) gauge error in dot line with square (...□...) and cross (...×...) symbols, respectively. The total gauge error ($\sqrt{\epsilon_{g-inst}^2 + \epsilon_{rep}^2}$) is represented by the simple dot line; (e) the radar errors (ϵ_{rad}) for the two radar algorithms and the gauge error ($\sqrt{\epsilon_{g-inst}^2 + \epsilon_{rep}^2}$); (f) the nugget parameter of the point correlation function. On the x-axis the rain threshold (in mm/h) applied on the data set.

When the radar reflectivity is corrected from the attenuation, the rain estimates shows no bias (Figure 3.c). Using the ZPHI® algorithm causes the bias to be slightly negative (-0.9) and remains constant when considering the various rain thresholds

The instrumental and representativeness gauge errors are presented in Figure 3.d. The gauge instrumental error decreases from 9% to 4% when the rain threshold increases. The representativeness error (ϵ_{rep}) is close to 20% when associated to a nugget parameter ranging from 1 to 0.94.

The radar error with the attenuation corrected “Z_c-R” algorithm is about 40%. The ZPHI® algorithm, which includes the attenuation correction, finally leads to an error of 25%, which approaches that of the gauge (Figure 3.e).

Habib and Krajewski (2002) quantified the contribution of gauge representativeness error associated with an area of 2km by 2km square and 15 min rain accumulation. The contribution of the variance of the gauge error to the variance of radar-gauge differences is found to be around (30%-45%) for light rain and (40%-75%) for heavy rain. In our study, $Var(r-R)/Var(R_g-R_{rad})$ is in the order of (30%-40%) when considering R_{rad} the rain estimated by ZPHI®. However the integration time and area difference make it difficult for the results to be fully comparable.

6. CONCLUSIONS

One of the objectives of the experiment was to validate the rainfall measured by the “Hydrix+ZPHI” radar system, compared with that measured by a network of 25 rain gauges. The results presented in this paper show a reasonably good agreement between the ZPHI®-derived radar rainfall and the gauge measurements. The benefits of ZPHI® in correcting rain “attenuation” and in adjusting the retrieval from DSD “variability” were analyzed and quantified.

The rain variability derived from the radar was compared to that measured by the gauge network, by computing the spatial correlation function. When using the standard Z-R relationship, the spatial correlation drops more rapidly, than that derived from the gauge network. Gebremicheal and Krajewski (2004) interpreted similar observations as significant that the radar provides a deteriorated information with respect to the rain gauge network. The correlation function obtained with the polarimetric algorithm ZPHI® improves significantly this picture: the radar derived correlation function really is really close to that from the gauges. However, it should be noticed that the scanning strategy of the radar and the location of the rain gauge network were particularly favorable in the Boigneville experiment.

From the radar alone, thanks to the large number of available samples, an accurate correlation function may be derived from a single rain event. Thus, the influence of time accumulation or type of events (stratiform-convective) can be studied. The correlation radius of intense rain events was found in some instance as small as 2 km, for 6 min integration time.

When comparing radar and gauge rain data, for validation purpose, the various error sources (instrumental and representativeness) should be considered. A new approach has been proposed, to

estimate these errors, which allows coexistence of a multiplicative error for the radar, an absolute error for the rain gauge, and a representativeness error (between point measurement and 1 km² pixel average) derived from the correlation function.

It was found, based on a one year rainfall data base, that the representativeness error is about 20%, while the gauge instrumental error ranges from 9 to 5%. The radar error depends on the algorithm used to derive the rain, with an error of 25% with ZPHI@, an error of 45% with a classical Z_c-R relationship (with Z_c corrected for attenuation).

Acknowledgements

The authors would like to thank the French research ministry for his support to the CITRAM project and ARVALIS-Institut-du-Végétal for providing rain gauge data.

References

Ciach G.J. and W.F. Krajewski, On the estimation of radar rainfall error variance, *Advances in Water Resources*, 1999, **22(6)**, 585-595.

Gebremichael M. and W.F. Krajewski, Assessment of the statistical characterization of small-scale rainfall variability from radar: analysis of TRMM ground validation Datasets, *Journal of Applied Meteorology*, 2004, **43**, 1180-1199.

Habib E. and W.F. Krajewski, Uncertainty analysis of the TRMM ground-validation radar-rainfall products: application to the TEFLUN-B Field campaign, *Journal of Applied Meteorology*, 2002, **41**, 558-572.

Krajewski W.F., G.J. Ciach and E. Habib, An analysis of small-scale rainfall variability in different climatic regimes, *Hydrological Sciences*, 2003, **48(2)**, 151-162.

Moreau E., J. Testud, E. Le Bouar, Rainfall spatial variability observed by X-band weather radar and its implication for the accuracy of rainfall estimates, *Advances in Water Resources*, 2009, **32(7)**, pp. 1011-1019.

Testud J., E. Le Bouar, E. Obligis and M. Ali-Meheni, The rain profiling algorithm applied to polarimetric weather radar. *J. Atmos. Oceanic Technol.*, 2000, **17**, 332-356.

Testud J., S. Oury, R.A. Black, P. Amayenc and X. Dou, The concept of "normalized" distribution to describe raindrop spectra: a tool for cloud physics and cloud remote sensing, *Journal of Applied Meteorology*, 2001, **40**, 1118-1140.